

Characterization of Two Types of Cesium-Bearing Microparticles (CsMPs) Emitted from the Fukushima Nuclear Power Plant Accident Using Multiple Synchrotron Radiation Analyses

Cesium-bearing microparticles (CsMPs), glassy radiocesium-enriched particles, were emitted from the Fukushima Daiichi Nuclear Power Plant accident. These CsMPs were isolated from environmental samples and analyzed by using micro-X-ray fluorescence analysis for various elements at BL-4A. The result shows a relationship between shape and concentration of volatile and refractory elements in the CsMPs, providing some implications on the formation and emission processes of CsMPs and the conditions in the reactor at the time of the accident.

In March 2011, large amounts of radionuclides were released into the environment by the Fukushima Daiichi nuclear power plant (FDNPP) accident [1]. Some of the radiocesium (Cs) was incorporated in Cs-bearing microparticles (CsMPs) mainly consisting of silica (SiO_2) [2]. Two main types of CsMP have been found thus far. One is called Type-A CsMP, which is spherical with a diameter $\sim 0.1\text{--}10\ \mu\text{m}$ and $\sim 10^2\text{--}10^4\ \text{Bq }^{137}\text{Cs}$ radioactivity per particle, and was emitted from Unit 2 or 3 of FDNPP. In contrast, Type-B CsMP has various shapes of $50\text{--}400\ \mu\text{m}$ diameter and $10^1\text{--}10^4\ \text{Bq}$ ^{137}Cs (Bq/particle), and was emitted from Unit 1. The chemical properties of these radioactive particles have been reported in detail, but in the previous studies, only a small number of particles were investigated, especially in the case of Type-B CsMPs. In this study, we endeavored to understand the radioactive particles systematically by analyzing a large number of particles [3].

As for CsMPs, road dust samples and other materials were collected at more than 100 sites within 50 km of FDNPP during 2011–2012. Sixty-seven CsMP samples were isolated in three steps [3]. First, the spatial distribution of radioactive Cs in the samples was measured by autoradiography with imaging plates to identify

CsMPs. Second, the wet separation method [4–6] was employed to isolate CsMPs from the samples containing CsMPs. After the isolation, the CsMPs in water used for the separation were carefully dropped on Kapton tape and air-dried for scanning electron microscopy (SEM) with energy-dispersive spectrometer (EDS) analysis to finally identify CsMPs on the basis of shape and elemental composition. For the Type-B CsMPs, micro-X-ray computed tomography (X-ray CT) analysis was conducted at SPring-8 BL37XU and 2D micro-X-ray fluorescence (XRF) measurement for various elements was conducted at BL-4A of Photon Factory, KEK [3].

X-ray CT results for Type-B CsMPs show a number of voids in their structures possibly related to gas release during their cooling processes. Although it is difficult to determine the volume of Type-B CsMPs from the external shape, X-ray CT analysis enabled us to accurately calculate the volume of internal voids. On the other hand, the volume of Type-A CsMPs was calculated from the apparent diameter, since we can assume a spherical shape on the basis of transmission electron microscopy (TEM) observations reported thus far [2]. **Figure 1** shows the relationship between ^{137}Cs radioactivity and volume for Types-A and -B CsMPs. As

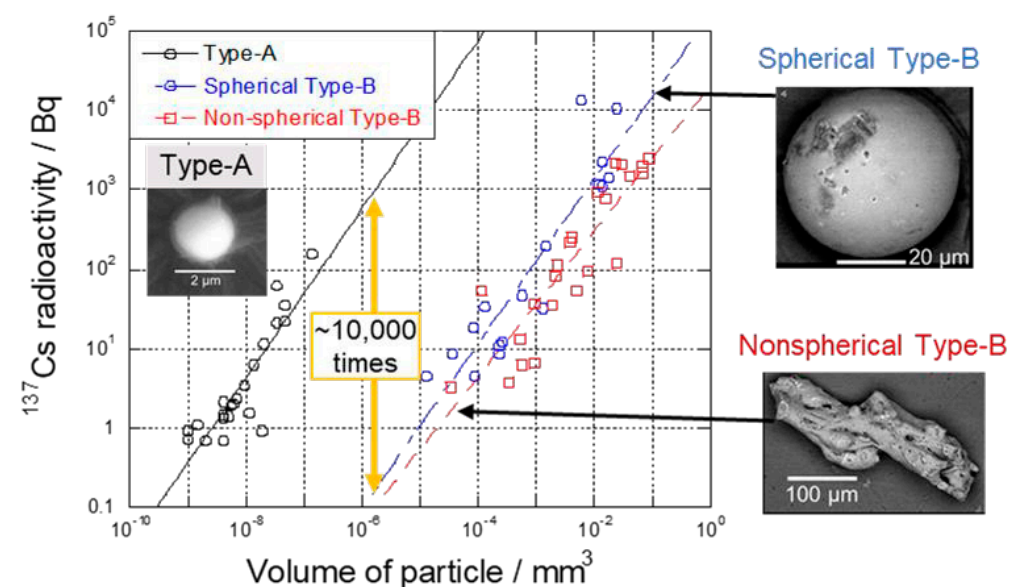


Figure 1: Relationship between ^{137}Cs radioactivity and volume of each CsMP.

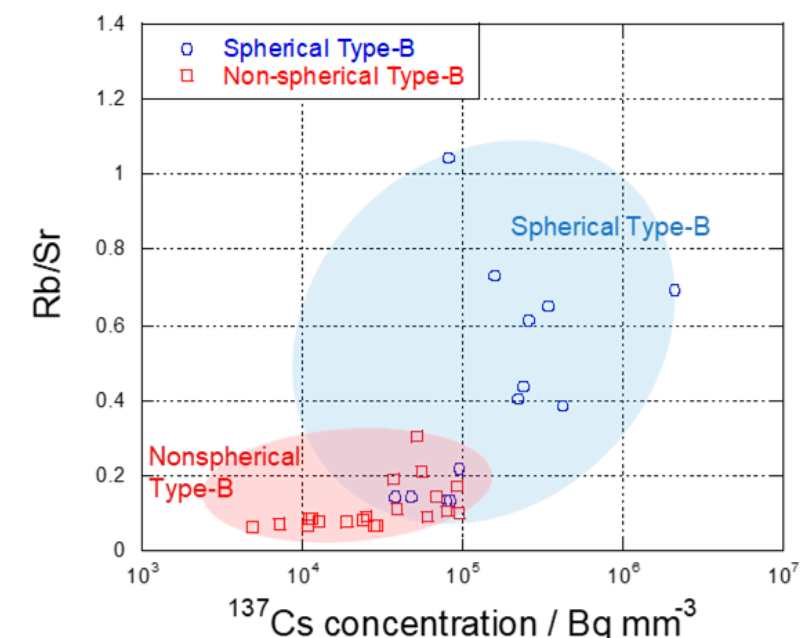


Figure 2: Relationship between ^{137}Cs concentration and XRF intensity ratio of Rb/Sr for each CsMP.

a result, the ^{137}Cs concentration per volume (Bq/mm^3) of Type-A CsMPs was $\sim 10,000$ times higher than that of Type-B CsMPs. Among the Type-B CsMPs, the spherical ones had higher concentrations of volatile elements such as ^{137}Cs than the nonspherical ones. These differences suggest that Type-A CsMPs were formed through gas condensation, whereas Type-B CsMPs through melt solidification. It is expected that (i) the ^{137}Cs concentration per volume of Type-A CsMP will be higher than that of Type-B CsMP, and (ii) that of spherical Type-B CsMP will be higher than that of nonspherical Type-B CsMP, since ^{137}Cs in Type-B CsMP is diluted by structural materials to a greater degree, particularly in nonspherical Type-B CsMP. These differences reflect the generation processes of Type-A and two types of Type-B CsMPs.

To support the hypothesis, XRF analysis was conducted particularly for rubidium (Rb) and strontium (Sr), since their X-ray fluorescence lines (Rb, $K_{\alpha 1}$: 13.4 keV; Sr, $K_{\alpha 1}$: 14.1 keV) were at high energies, which are not subject to the self-absorption effect. Since the matrix of CsMPs is SiO_2 , the attenuation length was larger than $500\ \mu\text{m}$ at X-ray energies above 13 keV. Therefore, Rb and Sr were analyzed with high-energy XRF, which also represented volatile and refractory elements, respectively. As expected from the volatility of these elements, spherical Type-B CsMPs had a higher Rb/Sr ratio than nonspherical Type-B CsMPs (**Fig. 2**). The Rb/Sr ratio in the spherical Type-B CsMPs increased with ^{137}Cs concentration, showing that spherical Type-B CsMPs have a higher concentration of volatile elements including Cs, than nonspherical Type-B CsMPs. Similar results were also found for antimony-125 (^{125}Sb), another volatile radionuclide emitted from FDNPP.

Consequently, this study provided chemical and morphological characteristics of 67 CsMPs, the number of which is larger than in previous CsMP studies, which usually dealt with fewer than 10 particles. In addition, systematic variations found in the relationships of ^{137}Cs radioactivity with the (i) volume of CsMP, (ii) porosity, (iii) Rb/Sr ratio, and (iv) ^{125}Sb activity allowed us to present some ideas regarding the formation and emission of CsMPs: (i) the condensation of gaseous species and melt solidification are the main processes for Types-A and -B CsMPs, respectively, and (ii) spherical particles had higher ^{137}Cs and ^{125}Sb concentrations and Rb/Sr ratios than nonspherical particles, possibly owing to the rapid cooling process, which inhibits the loss of volatile species during cooling.

REFERENCES

- [1] N. Yoshida and Y. Takahashi, *Elements* **8**, 201 (2012).
- [2] Y. Igarashi, T. Kogure, Y. Kurihara, H. Miura, T. Okumura, Y. Satou, Y. Takahashi and N. Yamaguchi, *J. Environ. Radioact.* **205**, 101 (2019).
- [3] H. Miura, Y. Kurihara, M. Yamamoto, A. Sakaguchi, N. Yamaguchi, O. Sekizawa, K. Nitta, S. Higaki, D. Tsumune, T. Itai and Y. Takahashi, *Sci. Rep.* **10**, 11421 (2020).
- [4] H. Miura, Y. Kurihara, A. Sakaguchi, K. Tanaka, N. Yamaguchi, S. Higaki and Y. Takahashi, *Geochem. J.* **52**, 145 (2018).
- [5] Y. Kurihara, N. Takahata, T. D. Yokoyama, H. Miura, Y. Kon, T. Takagi, S. Higaki, N. Yamaguchi, Y. Sano and Y. Takahashi, *Sci. Rep.* **10**, 3281 (2020).
- [6] H. Miura, T. Ishimaru, Y. Ito, Y. Kurihara, S. Ootaka, A. Sakaguchi, K. Misumi, D. Tsumune, A. Kubo, S. Higaki, J. Kanda and Y. Takahashi, *Sci. Rep.* **11**, 5664 (2021).

BEAMLINE

BL-4A

H. Miura¹ and Y. Takahashi² (¹CRIEPI, ²The Univ. of Tokyo)